Geometrical phases of excitonic qubits in quantum dots

2009 J. Phys.: Condens. Matter 21 045504

(http://iopscience.iop.org/0953-8984/21/4/045504)

IOP PUBLISHING JOURNAL OF PHYSICS: CONDENSED MATTER

J. Phys.: Condens. Matter **21** (2009) 045504 (8pp) doi:10.1088/0953-8984/21/4/045504

Geometrical phases of excitonic qubits in quantum dots

A Thilagam

Department of Physics, The University of Adelaide, 5005, Australia

E-mail: thilaphys@gmail.com

Received 17 September 2008, in final form 28 November 2008
Published 19 December 2008
Online at stacks.iop.org/JPhysCM/21/045504

Abstract

We investigate the influence of phonon mediated interactions on the non-unitary evolution of geometrical phases in excitonic qubits formed in quantum dots entangled by pure Förster coupling. We consider decoherence to occur via acoustic phonons interacting through the deformation potential and piezoelectric coupling mechanisms. The influences of bath temperature, external electric field, quantum dot size and interdot distance on the evolution of geometrical phases are examined for the GaAs/AlGaAs material system. We extend the theory to determine the effect of dynamic decoupling employing ultrafast π-pulses on the evolution of geometrical phases in the presence of dephasing processes.

1. Introduction

Exciton-based interactions in quantum dots play a vital role in the solid state implementation of quantum logic gates [1–4]. Excitons have an advantage over other forms of two-level systems in that they couple well with photons and have large dipole moments which allows easy manipulation of qubits via optical pulses [5]. Recent advances in creating and probing excitonic states [4, 6, 7] have provided rapid progress in the field of solid state quantum computation. The first observation of Rabi oscillations [8] in quantum dot excitons has demonstrated the ease with excitonic qubits can be manipulated as solid state logic gates. Despite these attractive features, excitonic qubits are subjected to undesirable effects of decoherence due to environmental factors such as lattice vibrations. In this work, we examine the key obstacles to the realization of geometric phase logic gates in exciton-based systems.

Several strategies such as decoherence-free subspaces [9, 10], optimal control techniques [11] and immunization processes [12] have been proposed to counter the detrimental effects of decoherence. One such proposal, geometric quantum computation has gained increased status as a robust fault-tolerant scheme [13–15] in recent years. The early works of Berry [16] showed that besides the usual dynamical phase, an additional phase known as the geometric phase is acquired by quantum systems which undergo adiabatic evolution. This geometric phase component relies solely on the Hilbert space geometry of the path executed during cyclical evolution and thus gives a measure of the curvature of the Hilbert space. The geometrical phase is therefore manifestly gauge invariant and generally considered to be robust against decoherence and stochastic operation errors [17].

Since the initial discovery by Berry in the mid-eighties [16], geometrical phases have been generalized to include non-adiabatic, non-cyclic and non-unitary evolutions of quantum systems [18–20]. Studies [21, 22] of the geometrical phase in composite systems have shown their critical dependence on the strength of coupling between the two subsystems and lattice temperature. A wide range of universal logic operations can be implemented by utilizing the unique properties of geometric phases of qubit systems manipulated via external controls [23]. Geometrical phase gates as logic systems using superconducting electron boxes in Josephson junction nanocircuits were studied in [14]. As pointed out by the authors of [14], advances in fabrication techniques allow implementation of conditional geometric phases in which the state of a neighbouring qubit determines the geometric phase of a qubit. Such a property is a key ingredient of quantum computing systems. Recent experimental measurements of geometrical phases in superconducting qubit systems [24] and Cooper pair pump [25] highlights the possibility of using geometrical phases to implement quantum logic processes in real physical systems.

Several works have investigated the effect of the external environment on the geometrical phase of quantum systems. The work by Whitney *et al* [26] showed that the geometrical phase of a spin-1/2 qubit acquires a noise-induced contribution

of geometrical origin as an external magnetic field precesses around the axis of a cone. An intuitive approach [27] to the effect of classical and quantum noise on the geometrical phase revealed the association of a topological component with quantum noise. Earlier works [28, 29] investigating the influence of environmental influence on geometrical phase gates have shown that environmental noise can impose constraints on proper functioning of logic gates. However to date, there is no conclusive evidence showing the superiority of geometrical computational schemes over other quantum forms of quantum logic in terms of their resilience to environmental noise. In this work, we investigate the influence of phonon mediated interactions on the non-unitary evolution of the geometrical phase for the specific case of excitonic qubits in Förster coupled quantum dots [30]. We provide quantitative estimates of the deviation from the purely unitary evolution of the geometrical phase due to lattice vibrations. We are unaware of other detailed studies of the influence of phonon mediated interaction on geometrical phases of this specific two-level solid state system.

In the latter part of this work, we study the effect of π-pulses in the presence of decoherence on the evolution of geometrical phases of quantum systems. Viola *et al* [31] and Ban [32] first proposed that application of several successive ultrafast π-pulses effectively reduces pure dephasing of a two-level system interacting with its surrounding reservoir. The interaction between the qubit spin and boson reservoir is generally assumed to be linear in the amplitude of the boson field. This approach, also known as the dynamical decoupling approach is based on the time reversal of the decoherence process in a short-timescale (about 0.5 ps) which is comparable to the reservoir correlation time. Interestingly, Akira [33] had suggested two decades earlier that the reversibility of decay in the phonon wavevector gives rise to suppression in decoherence during π-pulsing. Efforts to enhance this scheme has grown rapidly in recent years due to the potential benefits in quantum information processing. The decoherence of excitonic system in semiconductors is generally investigated by the four-wave and six-wave mixing techniques [34]. One of the first experimental works on π-pulsing of excitons [35] has recently confirmed that ultra-short π pulse sequences can control and decrease decoherence effects. In our work, we specifically examine the effect of dynamical decoupling [35, 36] on the evolution of geometrical phases during the first cycle of π-pulsing. There has been relatively little focus in the literature on the effect of decoherence on geometrical phases during π-pulsing of two-level quantum systems.

This paper is organized as follows. In section 2 we discuss key concepts of excitonic qubits and interdot Förster tunnelling in quantum dots. In section 3 we briefly examine the phonon mediated processes that lead to pure dephasing of excitonic qubits as well as spontaneous emission processes that provide an alternative route to decoherence in quantum dot systems. In section 4, we evaluate the geometrical phase of the composite exciton system using a kinematic approach and present numerical results for the case of the GaAs/AlGaAs material system. In section 5, we study the effect of dynamic decoupling on the evolution of the geometrical phase in the presence of decoherence. We provide conclusions of our work in section 6.

2. Excitonic qubits in quantum dots

We consider two excitons in their ground states in adjacent coupled quantum dots located at $\boldsymbol{R}_a$ and $\boldsymbol{R}_b$. We assume the quantum dots to be shaped in the form of either cuboid boxes or quasi-two-dimensional disks in which the vertical confinement energies of charge carriers are larger than their lateral confinement energies. For simplicity we ignore spin effects as exchange interactions due to singlet excitons are generally very small [37]. We label the localized excitonic states as $|\boldsymbol{R}_a\rangle$ and $|\boldsymbol{R}_b\rangle$ and accordingly code the excitonic qubits states using these relative positions via the basis set $\{|\boldsymbol{L}\rangle, |\boldsymbol{R}\rangle\}$:

$$\begin{aligned} |\boldsymbol{L}\rangle &= |\boldsymbol{R}_a\rangle \otimes |\boldsymbol{0}\rangle_b \\ |\boldsymbol{R}\rangle &= |\boldsymbol{0}\rangle_a \otimes |\boldsymbol{R}_b\rangle, \end{aligned} \tag{1}$$

where the states $|\boldsymbol{0}\rangle_a$ and $|\boldsymbol{0}\rangle_b$, which correspond to the absence of excitons, denote the respective ground states of the quantum dots at $|\boldsymbol{R}_a\rangle$ and $|\boldsymbol{R}_b\rangle$.

We simplify this approach by considering a two-level system involving only the states $|\boldsymbol{L}\rangle$ and $|\boldsymbol{R}\rangle$, and work in the limit of a pure Förster coupling. The direct Coulomb interaction which causes the formation of the biexciton state $|\boldsymbol{R}_a\rangle|\boldsymbol{R}_b\rangle$ is neglected, and we also exclude the possibility of entangled states involving the vacuum state $|\boldsymbol{0}\rangle_a|\boldsymbol{0}\rangle_b$. These assumptions will simplify subsequent mathematical analysis of the geometrical phase in section 4. The two-level excitonic qubit Hamiltonian takes the form

$$\widehat{H}_{\mathrm{ex-qb}} = -\hbar \left(\frac{\Delta\Omega}{2}\sigma_z + F\,\sigma_x \right), \tag{2}$$

where the Pauli matrices are given by $\sigma_x = |\boldsymbol{L}\rangle\langle\boldsymbol{R}| + |\boldsymbol{R}\rangle\langle\boldsymbol{L}|$ and $\sigma_z = |\boldsymbol{L}\rangle\langle\boldsymbol{L}| - |\boldsymbol{R}\rangle\langle\boldsymbol{R}|$, and $\Delta\Omega = \Omega_a - \Omega_b$ denotes the difference in exciton creation energy between the quantum dot at $\boldsymbol{R}_a$ and that at $\boldsymbol{R}_b$. F denotes the interdot Förster interaction amplitude responsible for the transfer of an exciton from one quantum dot to the other without involving a tunnelling process. The symmetric and antisymmetric eigenstates of this interacting qubit system are given by $|\chi_{\mathrm{s}}\rangle = \cos\frac{\beta}{2}|\boldsymbol{L}\rangle + \sin\frac{\beta}{2}|\boldsymbol{R}\rangle$ and $|\chi_{\mathrm{as}}\rangle = \sin\frac{\beta}{2}|\boldsymbol{L}\rangle - \cos\frac{\beta}{2}|\boldsymbol{R}\rangle$ with corresponding energies $E_{\mathrm{as(s)}} = \Omega_0 + \Omega_a - (\Delta\Omega/2) \pm \sqrt{(\Delta\Omega/2)^2 + F^2}$ where Ω_0 denotes the ground state energy of the system in which each quantum dot is unoccupied by excitons. The energy difference between the eigenstates is $\sqrt{\Delta\Omega^2 + (2F)^2}$ and in the absence of any decoherence, the excitonic qubit oscillates coherently between the two dots with the Rabi frequency $E_{\mathrm{as}} - E_{\mathrm{s}}$. The polar angle β in the Bloch sphere representation of a qubit is related to $\Delta\Omega$ and F by $\tan\beta = \frac{2F}{\Delta\Omega}$.

An explicit expression for the interdot Förster amplitude F is obtained by modelling the confining potentials of quantum charge carriers using harmonic potentials [40]

$$\begin{aligned} F(W) &= \langle\boldsymbol{R}|\widehat{H}_F|\boldsymbol{L}\rangle \\ &= \sqrt{\frac{11}{8}}\frac{\boldsymbol{\mu}\cdot\boldsymbol{\mu}}{\epsilon W^3}\left(\frac{2\ell_{\mathrm{e}}\ell_{\mathrm{h}}}{\ell_{\mathrm{e}}{}^2+\ell_{\mathrm{h}}^2}\right)^2\left(\frac{2\ell_{z\mathrm{e}}\ell_{z\mathrm{h}}}{\ell_{z\mathrm{e}}{}^2+\ell_{z\mathrm{h}}{}^2}\right), \end{aligned} \tag{3}$$

where the interdot distance $W = |\boldsymbol{R}_a - \boldsymbol{R}_b|$. The length scales ℓ_e and ℓ_h are associated with the respective electron and hole harmonic potentials in the lateral direction while those in the vertical direction are defined by ℓ_{ze} and ℓ_{zh} for electrons and holes, respectively. $\boldsymbol{\mu}$ denotes the interband dipole matrix element which can be obtained using experimental measurements [38].

In the presence of an external electric field E, equation (3) becomes modified as

$$F(W) = \sqrt{\frac{11}{8}}\frac{|\boldsymbol{\mu}|^2}{\epsilon W^3}\left(\frac{2\ell_e\ell_h}{\ell_e^2+\ell_h^2}\right)^3 \exp\left(-\frac{e^2E^2(c_e+c_h)^2}{2c_e^2c_h^2(\ell_e^2+\ell_h^2)}\right) \tag{4}$$

where we have assumed $\ell_{ze} = \ell_e, \ell_{zh} = \ell_h$. The parameters c_e and c_h are determined by the confining potential energies for electrons and holes, respectively [39]. In this work, we use typical values of $c_e \sim c_h = 5\times10^{-3}$ J m^{-2} to obtain numerical results in section 4.

3. Exciton–phonon interaction in quantum dots

We consider a simplified spin–boson model in which the Förster interaction is switched off after a certain time, which we set at $t = 0$. We consider the exciton state at each quantum dot to be coupled to a continuum of acoustic phonons via both the deformation potential and piezoelectric coupling. We assume that the interaction between the two-state excitonic qubit and surrounding phonon environment is linear so that the Hamiltonian of the system under study is given by

$$\widehat{H}_{qb}^{env} = \widehat{H}_{ex-qb} + \widehat{H}^{ph} + \widehat{H}_{ex-qb}^{DP} \tag{5}$$

where $\widehat{H}_{ex-qb}$ is given by equation (2), and $\widehat{H}^{ph}$ denotes the Hamiltonian for the phonon bath

$$\widehat{H}_{ph} = \sum_{\mathbf{q}} \hbar\omega_{\mathbf{q},\lambda}\, b_\lambda^\dagger(\mathbf{q})\, b_\lambda(\mathbf{q}), \tag{6}$$

where $b_\lambda^\dagger(\mathbf{q})$, and $b_\lambda(\mathbf{q})$, are the respective creation and annihilation operators of a λ-mode phonon with wavevector $\mathbf{q}$. The λ-mode is denoted LA for longitudinal acoustic phonons and TA for transverse acoustic phonons. The acoustic phonon energy spectrum is determined by the dispersion relation $\omega_{\mathbf{q},LA} = \upsilon_{LA}|\mathbf{q}|$ for the longitudinal mode and $\omega_{\mathbf{q},TA} = \upsilon_{TA}|\mathbf{q}|$ for the transverse mode, with υ_{LA} and υ_{TA} denoting the corresponding sound velocities. In order to simplify the approach, we consider phonon interactions at low bath temperatures so that coupling associated with optical phonons can be neglected.

$\hat{H}_{ex-qb}^{DP}$ is the excitonic qubit–phonon interaction Hamiltonian associated with deformation potential coupling

$$\hat{H}_{ex-qb}^{DP} = \sum_{\lambda,\mathbf{q}} \sqrt{\frac{\hbar|\mathbf{q}|^2}{2\rho\, V\, \omega_{\mathbf{q}\lambda}}} \mathrm{M_p}(\mathbf{q})\, \sigma_z \left(b_\lambda^\dagger(-\mathbf{q}) + b_\lambda(\mathbf{q})\right) \times |n_{\mathbf{q}\lambda}\rangle\langle n_{\mathbf{q}\lambda}| \tag{7}$$

where $|n_{\mathbf{q}\lambda}\rangle$ denotes the occupation number of λ-mode phonon with wavevector, $\mathbf{q}$. V is the crystal volume and ρ is the mass density of the material system. D_c and D_v are the respective deformation potential constants for the conduction and valence bands. $\hat{H}_{ex-qb}^{DP}$ commutes with σ_z, i.e $[\sigma_z, \hat{H}_{ex-qb}^{DP}] = 0$ so that a simplified model in which only the pure dephasing process with no dissipation effects is considered in this work. The term $\mathrm{M_p}(\mathbf{q})$ is given by

$$\mathrm{M_p}(\mathbf{q}) = \langle\chi_s; n_{\mathbf{q}\lambda} \pm 1|\left(D_c e^{i\,\mathbf{q}\cdot\mathbf{r_e}} - D_v e^{i\,\mathbf{q}\cdot\mathbf{r_h}}\right)|\chi_s; n_{\mathbf{q}\lambda}\rangle - \langle\chi_{as}; n_{\mathbf{q}\lambda} \pm 1|\left(D_c e^{i\,\mathbf{q}\cdot\mathbf{r_e}} - D_v e^{i\,\mathbf{q}\cdot\mathbf{r_h}}\right)|\chi_{as}; n_{\mathbf{q}\lambda}\rangle. \tag{8}$$

Details of evaluating an explicit expression for $\mathrm{M_p}(\mathbf{q})$ is provided in [40]. In subsequent calculations, we assume that $\ell_{ze} = \ell_e = \ell_{zh} = \ell_h \approx \ell$ to determine the decoherence function $\Gamma(t)$ (see equation (13) given below) associated with phonon coupling via deformation potential. It is important to note that in equation (8), we have considered that phonon-induced transitions between the symmetric and antisymmetric states contribute predominantly to the decoherence process. While scattering between other states occurs, the match between phonon with low energies and the small energy difference between $|\chi_{as}\rangle$ and $|\chi_s\rangle$ states is optimized at low enough temperatures.

The Hamiltonian $\hat{H}_{ex-qb,\lambda}^{Piez}$ describing exciton–phonon interaction via piezoelectric coupling is given by

$$\hat{H}_{ex-qb,\lambda}^{Piez} = \sum_{\lambda,\mathbf{q}} \frac{8\pi e e_{14}}{\epsilon_0\epsilon_r|\mathbf{q}|^2}\sqrt{\frac{\hbar}{2\rho\, V\, \omega_{\mathbf{q}\lambda}}} \times \left(\xi_{x,\lambda}q_yq_z + \xi_{y,\lambda}q_xq_z + \xi_{z,\lambda}q_xq_y\right) \times \mathrm{N_p}\,\sigma_z\left(b_\lambda^\dagger(-\mathbf{q}) + b_\lambda(\mathbf{q})\right)|n_{\mathbf{q}\lambda}\rangle\langle n_{\mathbf{q}\lambda}| \tag{9}$$

where the relative permittivity, ϵ_r is assumed to be unaffected by the contribution from strain fields associated with acoustic phonon modes. e_{14} is the piezoelectric constant and $\xi_{i,\lambda}$ is the unit vector of polarization of the λ-phonon along the i-direction. Excitonic interactions with phonons due to piezoelectric coupling are highly anisotropic in nature [42] and the form of $\hat{H}_{ex-qb,\lambda}^{Piez}$ depends on the choice of polarization components and the modes associated with λ. Using specific dependence of $\hat{H}_{ex-qb,\lambda}^{Piez}$ on LA, TA1 and TA2 modes [42], we can evaluate the corresponding terms $\mathrm{N_p}$ which has a form similar to $\mathrm{M_p}$ in equation (8). Unlike $\mathrm{M_p}$, $\mathrm{N_p}$ vanishes as $\mathbf{q} \to 0$ due to the exact cancellation of electron and hole form factors as the piezoelectric coupling constant is the same for both electron and hole. In subsequent calculations, we assume that $\ell_{ze} = \ell_e \approx \ell, \ell_{zh} = \ell_h, r = \ell_e/\ell_h$ to simplify evaluation of the decoherence function $\Gamma(t)$ associated with phonon coupling via piezoelectric coupling. At $r = 1$, the dephasing rates reduce to zero due to the piezoelectric coupling being a polar mechanism [40].

3.1. Exciton decay via spontaneous emission process

While our focus in this work is decoherence via phonon-induced transitions, exciton decay via spontaneous emission is also an important source of decoherence in quantum dot systems. Here we briefly examine how excitons which are Förster transferred are affected by recombination due to spontaneous emission associated with an external environment of photons. A crude estimate of the exciton lifetime can be obtained by using a simple model of a two-level quantum dot

exciton interacting with just a single mode of radiation at zero electric field

$$\frac{1}{\tau_{\rm d}} = \frac{\omega_o^3|\boldsymbol{\mu}|^2}{\hbar\pi^2 c^3\epsilon}\left(\frac{2\ell_{\rm e}\ell_{\rm h}}{{\ell_{\rm e}}^2+\ell_{\rm h}^2}\right)^2\left(\frac{2\ell_{ze}\ell_{z{\rm h}}}{{\ell_{ze}}^2+{\ell_{z{\rm h}}}^2}\right) \tag{10}$$

where ω_o is the exciton creation energy. For the GaAs/AlGaAs system, we use typical values of $\omega_o \sim 1.9$ eV, $|\boldsymbol{\mu}| \sim 5\ e$Å and $\ell_{\rm e} \approx \ell_{\rm h} = \ell_{ze} = \ell_{z{\rm h}}\ell = 1$ nm to obtain a rough estimate for the exciton lifetime, $\tau_{\rm d} \sim 300$ ps. This is almost comparable to estimates of the decoherence times of 10–100 ps associated with exciton–phonon interaction in excitonic qubits [40]. Hence we expect spontaneous emission processes to provide an important alternative route to decoherence besides those associated with phonon mediated interactions. Nevertheless in subsequent sections, we will focus just on phonons as providing the main source of decoherence during phase evolution for mathematical simplicity. We expect that exclusion of the spontaneous emission decay term in equation (10) will not affect the overall order of magnitude of the geometrical phase calculated using phonon related terms only.

4. Geometrical phase of the composite exciton system

Here we briefly summarize the main properties of geometric phases within the context of a two-level system like the exciton qubit in quantum dots. When a two-level excitonic qubit Hamiltonian undergoes cyclic evolution while driven by an external field **B**, the Bloch vector traces a closed path in the time interval $[0, T]$. This closed path exists in the projective Hilbert space of the Bloch sphere in which the north pole represents the $|\boldsymbol{L}\rangle$ state while the south pole represents the $|\boldsymbol{R}\rangle$ state. All other superpositions states lie on the surface of the Bloch sphere. The position of the vertex of the Bloch sphere is controlled by the polar angle β determined by parameters $\Delta\Omega$ and interdot Förster amplitude F. At the completion of one cycle in the parameter space **B**, the qubit state vector acquires a geometric phase other than a dynamic phase. This geometric phase which we denote as η_0 is given by the well-known value of half of the solid angle that the circuit path subtends at the point $\mathbf{B} = 0$ in the absence of environmental noise [16]. Thus if the excitonic qubit system undergoes a unitary evolution with cone angle β, $\eta_0 = \frac{1}{2}\Omega = -\pi(1-\cos\beta)$ where Ω is the solid angle subtended by the conical path. η_0 is not affected by the speed of cyclical evolution [16]. In the presence of dephasing and dissipation, evolution of η becomes non-unitary and is modified by the addition of a correction term $\eta_{\rm c}$ to η_0. In this work, we evaluate the modified geometrical phase of the composite exciton system $\eta = \eta_0 + \eta_{\rm c}$ using the kinematic approach of Oh *et al* [18, 19]. This approach is suitable for two-level systems undergoing both dephasing and dissipation due to external noises.

The interacting exciton–phonon system in equation (5) satisfies the Schrödinger equation

$$\mathrm{i}\frac{\partial|\chi_t\rangle}{\partial t} = \widehat{H}_{\rm qb}^{\rm env}|\chi_t\rangle, \tag{11}$$

where $\widehat{H}_{\rm qb}^{\rm env}$ is given by equation (5) and the state vector $|\chi_t\rangle$ is given by a linear combination of the product of excitonic qubit and phonon states. We consider an initial state given by

$$|\chi_{\rm s}\rangle = \cos\frac{\beta_0}{2}|\boldsymbol{L}\rangle + \sin\frac{\beta_0}{2}|\boldsymbol{R}\rangle.$$

At $t = 0$, $|\chi_{\rm s}(0)\rangle$ depends on the interdot Förster interaction amplitude F through the angle $\beta_0 = \beta(0)$. The evolution of β with time depends on the dynamics of the interaction between the qubit states and the phonon bath. At $t = 0$, the reduced density matrix is given by $\rho_0 = |\chi_{\rm s}(0)\rangle\langle\chi_{\rm s}(0)|$. At times $t > 0$, the density matrix $\rho_T = |\chi_{\rm s}\rangle\langle\chi_{\rm s}|$ evolves according to

$$\rho_T(t) = \begin{pmatrix} \cos^2\frac{\beta(t)}{2} & \frac{1}{2}\sin\beta(t)\,\mathrm{e}^{\mathrm{i}t\Delta\Omega}Z \\ \frac{1}{2}\sin\beta(t)\,\mathrm{e}^{-\mathrm{i}t\Delta\Omega}Z & \sin^2\frac{\beta(t)}{2}\end{pmatrix}, \tag{12}$$

where $\Delta\Omega$ denotes the difference in exciton creation energy between the two quantum dots (also known as bias) and $Z(t) = \mathrm{e}^{-4\Gamma(t)}$ gives a measure of the decay of the off-diagonal matrix elements in the presence of a phonon bath. The decoherence term $\Gamma(t)$ has the well-known form [43]

$$\Gamma(t) = \int\frac{\mathrm{d}\omega}{\hbar\omega^2}J_{\rm X}(\omega)\coth\left(\frac{\hbar\omega}{2k_{\rm B}T}\right)\sin^2\frac{\omega t}{2}, \tag{13}$$

where X = DP or Piez and $J_{\rm X}(\omega)$ is the spectral density function which yields information about the interaction of the quantum dot with phonons

$$\begin{aligned} J_{\rm DP}(\omega) &= \sum_{\mathbf{q}}{\rm M_p}(\mathbf{q})^2\delta(\omega-\omega_{\mathbf{q}}) \\ J_{\rm Piez}(\omega,\lambda) &= \sum_{\mathbf{q}}{\rm N_p}(\mathbf{q})^2\delta(\omega-\omega_{\mathbf{q}}), \end{aligned} \tag{14}$$

where $\mathrm{M_p}(\mathbf{q})$ is given in equation (8). $\mathrm{N_p}(\mathbf{q})$ associated with phonons which interact via piezoelectric coupling can be obtained in similar form as equation (8). At small ω, $J(\omega) \sim \omega^k$ where the exponent k distinguishes the cases of ohmic ($k = 1$), sub-($k < 1$) and super-ohmic ($k > 1$) couplings [43]. The angle β in equation (12) is also a function of t and is determined (for $t > 0$ only) by:

$$\tan\frac{\beta(t)}{2} = \mathrm{e}^{-\Gamma(t)}\cot\frac{\beta_0}{2}.$$

Following [18, 19], we define the geometrical phase η by $\eta = \arg z$ where

$$z = \sum_j\sqrt{E_j(0)E_j(T)}\langle\chi_j(0)|\chi_j(T)\rangle\mathrm{e}^{-\int_0^T\mathrm{d}t\langle\chi_j(t)|\dot{\chi}_j(t)\rangle}. \tag{15}$$

The system frequency $\Delta\Omega$ determines the quasi-cyclic path of the geometric phase, with time t varying from 0 to $T = \frac{2\pi}{\Delta\Omega}$. $E_j(T)$ and $\chi_j(T)$ refer to the eigenvalues and eigenvectors respectively of the density matrix ρ_T in equation (12), and (taking $j = \pm$)

$$\begin{aligned} E_\pm(t) &= \tfrac{1}{2} \pm \tfrac{1}{2}\left[\cos^2\beta(t) + \mathrm{e}^{-2\Gamma(t)}\sin^2\beta(t)\right]^{\frac{1}{2}}, \\ |\chi_+(t)\rangle &= \cos\frac{\beta(t)}{2}|\boldsymbol{R}\rangle + \mathrm{e}^{-\mathrm{i}t\Delta\Omega}\sin\frac{\beta(t)}{2}|\boldsymbol{L}\rangle. \end{aligned} \tag{16}$$

The time evolution of the phase is determined only by $|\chi_+(t)\rangle$ because $E_-(0) = 0$, where we also use $\Gamma(0) = 0$, $Z(0) = 1$ and $|\chi_+(0)\rangle = |\chi_s(0)\rangle$. By substituting equation (16) into equation (15) we find η takes the form $\eta = \eta_0 + \eta_c$ where $\eta_0 = -\pi(1 - \cos\beta_0)$. η_c which accounts for the non-unitary contributions due to a noisy environment is obtained using a series expansion of the dissipative term ϑ

$$\eta_c \approx \frac{\vartheta}{2\pi T}\int_0^T \mathrm{d}t\left[\frac{\partial\Gamma(t)}{\partial\vartheta}\right]_{\vartheta=0}. \tag{17}$$

Using equations (7) and (9), we derive approximate expressions for ϑ in terms of the environmental parameters for $\lambda = \mathrm{LA}$,

$$\begin{aligned}\vartheta_{\mathrm{DP}} &\approx \frac{(D_c - D_v)^2}{\rho\upsilon_{\mathrm{LA}}^2\ell^3}\\ \vartheta_{\mathrm{Piez}} &\approx \frac{e^2e_{14}^2}{\epsilon^2\rho\upsilon_{\mathrm{LA}}^2\ell}, \qquad (r > 1).\end{aligned} \tag{18}$$

Hence the correction term η_c disappears for $\vartheta_{\mathrm{DP}} = \vartheta_{\mathrm{Piez}} = 0$ and the phase evolves unitarily in the absence of external noise. The evaluation of η_c via equation (18) is justified as we consider the GaAs/AlGaAs material system in which the exciton–phonon interactions are weak and ϑ_{DP}, $\vartheta_{\mathrm{Piez}}$ have small values. Equation (15) is gauge invariant and can be viewed as the weighted sum of component geometrical phases with respect to eigenstates of the density matrix in equation (12).

We use parameters typical to the GaAs/AlGaAs material system [41] to calculate the geometrical phase η. Figures 1(a) and (b) show η as functions of bias $\Delta\Omega$ in the presence of decoherence due to coupling with phonons via deformation potential and piezoelectric coupling, respectively. The initial state of entanglement is encoded in the angle β_0 which provides a measure of strength of entanglement between $|\boldsymbol{L}\rangle$ and $|\boldsymbol{R}\rangle$ states. The geometrical phase η_0 increases with the strength of entanglement and with β_0 until the maximum value of $\eta_0 = \pi$ is reached at $\beta_0 = \frac{\pi}{2}$. This explains the monotonic decrease in $|\eta_0|$ (full lines) with $\Delta\Omega$. In subsequent figures, we note a similar trend of η_0 changing with other external parameters like electric field E and interdot distance W.

Figures 1(a) and (b) also show the well-known increase of decoherence effects with bath temperature which leads to the suppression of η at higher temperatures, in agreement with previous works [29]. Comparison of figures 1(a) and (b) shows that the departure from unitary behaviour occurs more at lower values of $\Delta\Omega$ where there is a greater degree of entanglement between the $|\boldsymbol{L}\rangle$ and $|\boldsymbol{R}\rangle$ states. This feature is more marked in the case of phonon coupling via deformation potential compared to coupling via the piezoelectric mechanism due to the difference in strength and nature of spectral density function associated with the two modes of coupling mechanisms.

At $T = 0$ K, zero point fluctuations associated with a noisy environment contribute to the correction term η_c. It can be seen that such fluctuations make a sizable contribution to non-unitary evolution at low bias $\Delta\Omega$. At very low temperatures, the quantum-thermal timescale is given by

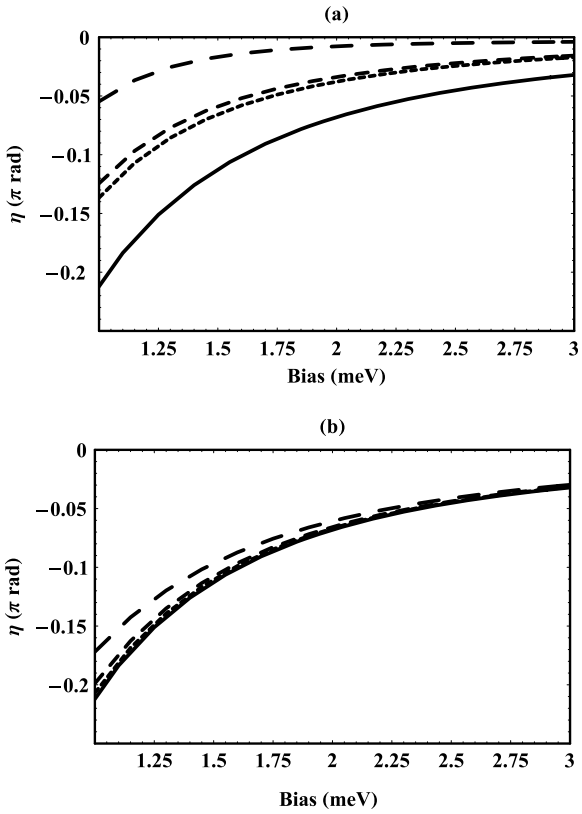

Figure 1. (a) Geometrical phase η (in units of π radians) as a function of bias $\Delta\Omega$ in the presence of decoherence due to coupling with phonons via deformation potential at $W = 5$ nm, $\ell_e \approx \ell_h = \ell = 1$ nm, electric field $E = 0$ MV m^{-1} and $T = 35$ K (long dashed), 10 K (short dashed), $T = 0$ K (dotted) and unitary evolution with no decoherence (full). (b) Geometrical phase η as a function of bias $\Delta\Omega$ in the presence of decoherence due to coupling with phonons via piezoelectric mechanism at $W = 5$ nm, $\ell_{ze} = \ell_e \approx \ell = 1$ nm, $r = \ell_e/\ell_h = 5$, electric field $E = 0$ MV m^{-1} and $T = 35$ K (long dashed), 10 K (short dashed), $T = 0$ K (dotted) and unitary evolution with no decoherence (full).

$T_{\mathrm{th}} = \hbar/k_BT$ and becomes very large compared to the cut-off frequency $\omega_c \sim \upsilon_{\mathrm{LA}}/\ell$;. ω_c is the cut-off frequency beyond which $J_X(\omega)$ decreases to zero and is determined by the approximate phonon flight time through the quantum dot which is ∼0.5 ps for the case of the GaAs/AlGaAs material system. With the loss of one timescale at $T = 0$, we expect bath correlations to play a critical role in the quantum dynamical interactions in the femtosecond timescale.

Figures 2(a) and (b) show that external electric field E has similar effects on η as bias $\Delta\Omega$. An increase in E results in a monotonic decrease in the interdot Förster interaction amplitude F. This decreases the strength of entanglement between the $|\boldsymbol{L}\rangle$ and $|\boldsymbol{R}\rangle$ states and consequently $|\eta_0|$ decreases. Figures 2(a) and (b) show the larger suppression of the geometrical phase and hence greater departure from unitary evolution due to increasing temperatures at small electric field values. The figures also show the disparity in the response of η to an external electric field between the two modes of phonon coupling mechanisms.

Decoherence increases with decreasing quantum dot size ℓ as can be noted in the dissipative term ϑ (equation (18)).

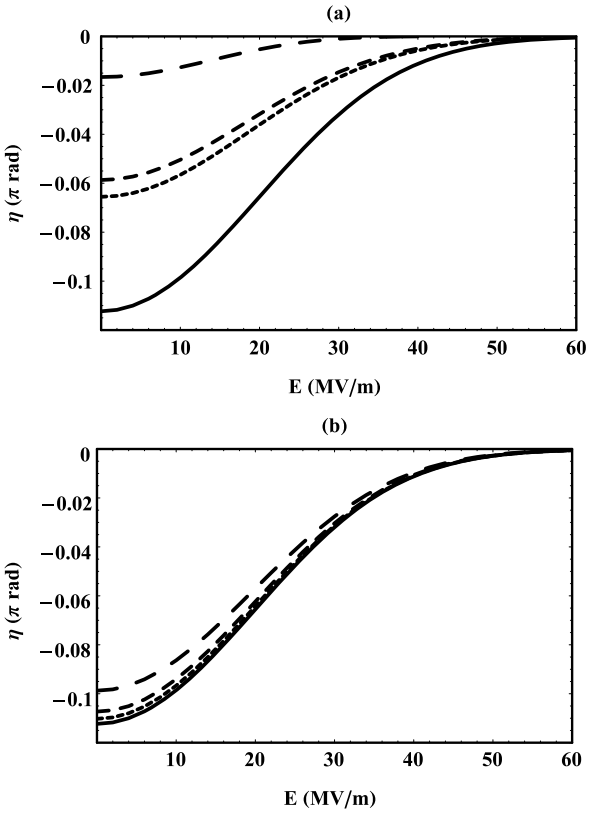

Figure 2. (a) Geometrical phase η as a function of external electric field E in the presence of decoherence due to coupling with phonons via deformation potential at $\Delta\Omega = 1.5$ meV, $W = 5$ nm, $\ell_e \approx \ell_h = \ell = 1$ nm and $T = 30$ K (long dashed), 10 K (short dashed), $T = 0$ K (dotted) and unitary evolution with no decoherence (full). (b) Geometrical phase η as a function of external electric field E in the presence of decoherence due to coupling with phonons via piezoelectric mechanism at $\Delta\Omega = 1.5$ meV, $W = 5$ nm, $\ell_{ze} = \ell_e \approx \ell = 1$ nm, $r = \ell_e/\ell_h = 5$, and $T = 35$ K (long dashed), 10 K (short dashed), $T = 0$ K (dotted) and unitary evolution with no decoherence (full).

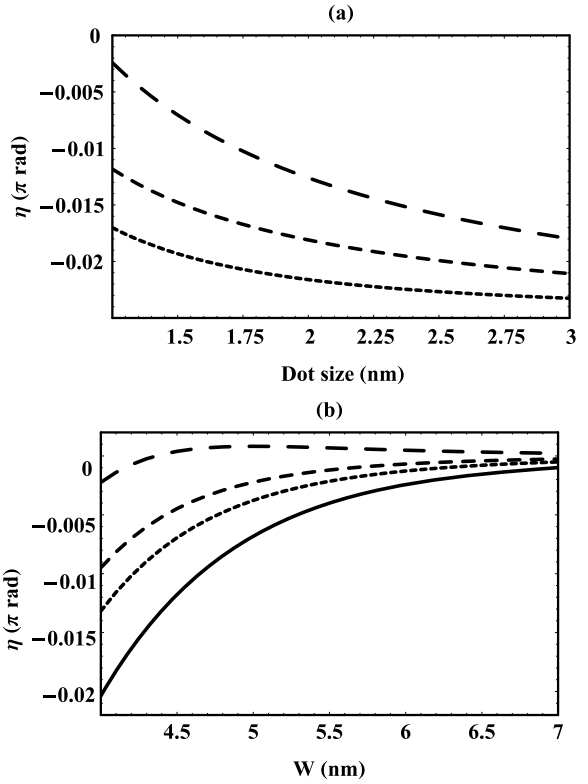

Figure 3. (a) Geometrical phase η as a function of quantum dot size $\ell_e \approx \ell_h = \ell$ in the presence of decoherence due to coupling with phonons via deformation potential at $\Delta\Omega = 2$ meV, $W = 6$ nm, electric field $E = 0$ MV m^{-1} and $T = 40$ K (long dashed), 20 K (short dashed), $T = 0$ K (dotted). (b) Geometrical phase η as a function of interdot distance W in the presence of decoherence due to coupling with phonons via deformation potential at $\Delta\Omega = 2$ meV, $\ell_e \approx \ell_h = \ell = 1$ nm, electric field $E = 0$ MV m^{-1} and $T = 40$ K (long dashed), 20 K (short dashed), $T = 0$ K (dotted).

Therefore suppression of the geometrical phase η is large at small ℓ as shown in figure 3(a) for exciton–phonon interaction via deformation potential. This suppression is further enhanced at higher temperatures. These features can also be obtained in the case of piezoelectric mechanism but are expected to be less marked.

An increase in the interdot distance W results in a decrease in the strength of entanglement between the $|\boldsymbol{L}\rangle$ and $|\boldsymbol{R}\rangle$ states. Thus $|\eta_0|$ decreases with an increase in W as shown in figure 3(b). The figure also shows that increasing the bath temperature causes departure from unitary evolution at small values of W. The results shown in figures 1(a)–3(b) highlight the critical role of the bath temperature, external electric field E and quantum dot parameters ℓ and W in influencing the properties of geometric phases in excitonic qubit systems. These same parameters also have a strong influence on the behaviour of zero point fluctuations in the limit where temperature becomes zero. This information may be useful in reducing phonon-assisted decoherence via careful choice of system parameters in order to realize higher fidelity in logic gate operations.

5. Effect of dynamic decoupling on the evolution of the geometrical phase in the presence of decoherence

We consider the case of an excitonic qubit that is subjected to two successive optical π pulses of femtosecond duration [35]. The first π-pulse rotates the qubit state vector through an angle π about the x-axis while the second pulse inverts the state vector back to its initial state. Under the action of two π-pulses, the initial excitonic state acquires an overall phase of π, provided decoherence mechanisms are absent. We assume that the important effect of reversal of time evolution of the qubit system is achieved during the bit-flipping of qubit vectors. This is justified for pulses of very short duration which is of the same order of magnitude as phonon interaction and decay times in the non-Markovian dynamics regime [35]. To simplify the model, we ignore exciton–phonon interaction *while* the decoupling pulses are switched on. This assumption is justified as the pulses exist for very short times compared to the decoherence times (≈10–100 ps) associated with exciton–phonon interaction in excitonic qubits [40].

The Hamiltonian representing the dynamic decoupling pulses is written as [31, 44]

$$\hat{H}_{\rm pul} = \sum_{n=1}^{N} V_n(t) \mathrm{e}^{\mathrm{i}\frac{\Delta\Omega}{2}t\sigma_z}\sigma_x \mathrm{e}^{-\mathrm{i}\frac{\Delta\Omega}{2}t\sigma_z} \qquad (19)$$

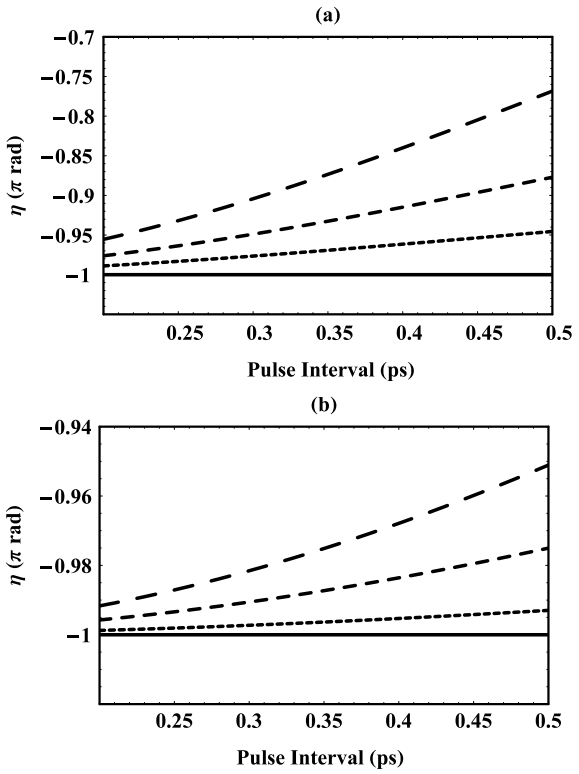

Figure 4. (a) Geometrical phase η as a function of pulse interval Δt in the presence of decoherence due to coupling with phonons via deformation potential at $\ell_e \approx \ell_h = \ell = 1$ nm, $W = 6$ nm, and $T = 120$ K (long dashed), 60 K (short dashed), $T = 0$ K (dotted) and unitary evolution with no decoherence (full). (b) Geometrical phase η as a function of pulse interval Δt in the presence of decoherence due to coupling with phonons via piezoelectric mechanism at $\ell_{ze} = \ell_e \approx \ell = 1$ nm, $r = \ell_e/\ell_h = 5$, $W = 6$ nm, and $T = 120$ K (long dashed), 60 K (short dashed), $T = 0$ K (dotted) and unitary evolution with no decoherence (full).

where a periodic sequence of N equidistant ideal π-pulses are applied at times $t_N = N\Delta t$. Δt denotes the inter-pulse separation time and $T_v = 2\Delta t$ is one cycle duration in the dynamic decoupling process. In the presence of the dynamic decoupling Hamiltonian in equation (19), the decoherence function $\Gamma(t)$ in equation (13) becomes modified [31]

$$\Gamma_v(t) = \int \frac{\mathrm{d}\omega}{\hbar\omega^2} J_X(\omega) \coth\left(\frac{\hbar\omega}{2k_B T}\right) \sin^2\frac{\omega t}{2} \tan^2\frac{\omega\Delta t}{2}, \tag{20}$$

where time $t = NT_v$. The term $\tan^2\frac{\omega\Delta t}{2}$ which appears as a result of the dynamic decoupling pulses suppresses decoherence at low frequencies provided the relation $\omega_c \Delta t \leqslant \pi$ is satisfied. At non-zero temperatures, the fastest timescale of the environment is given by $(1/\omega_c)$ with the dynamic decoupling pulses acting as a *high-pass filter* [44] for quantum noise associated with the surrounding bath of phonons.

In order to obtain numerical values for the GaAs/AlGaAs material system, we set the initial geometrical phase of the excitonic qubit to be $\eta_0 = -\pi(1 - \cos 0) = -\pi$. For the sake of simplicity, we assume $N = 2$ so that only a pair of π-pulses are considered. We consider the qubit state to begin dephasing *before* the arrival of the first π-pulse. After the arrival of two π-pulses, the qubit state acquires a corrective geometrical phase associated with the topological component of dephasing process besides a phase of $-\pi$. As mentioned earlier, the corrective geometrical phase serves to suppress the geometrical phase gained as a result of the dynamic decoupling pulses. After the arrival of the first π-pulse and prior to the arrival of the second π-pulse, the qubit has decohered for an extra $t = \Delta t$. Therefore the overall geometrical phase of the excitonic qubit is given by $\eta = -\pi + \eta_c$ where η_c can be used in the form given in equation (17) with $2\Delta t$ taken as the time required for one cycle duration.

Figures 4(a) and (b) show that the non-unitary contributions due to phonon mediated interactions (as quantified by η_c) increases with pulse interval Δt. This is due to more time available for decoherence effects at larger values of Δt. It is notable that decoherence due to thermal effects decreases significantly for $\Delta t \sim 0.1$ ps at bath temperatures as high as 120 K. The dynamic decoupling mechanism provided by the π-pulses are just as effective in reducing decoherence associated with zero point fluctuations in the lattice medium. Overall the figure illustrates the fact that as the pulse interval becomes smaller, the effectiveness of the pulse control increases which is consistent with results of earlier works [31, 35, 44].

It is to be noted that Markovian theory forms the basis of decoherence function $\Gamma(t)$ given in equations (13) and (20). These expressions are adequate in the semiclassical regime where small phonon correlation times with negligible memory effects are present. However when the inter-pulse separation time reaches values less than the phonon bath correlation times, we expect Markovian theories to fail and the exciton–phonon dynamics need to be modelled using a quantum kinetic formalism [45]. It is expected that interesting short-time system dynamics like phonon reservoir memory effects will be revealed within this model which examines the exciton–phonon interaction in terms of the retarded Green function and phonon particle propagator terms. This formalism is beyond the scope of our work and therefore we only consider inter-pulse separation times $\geqslant$0.1 ps which correspond roughly to the bath correlation time in GaAs/AlGaAs material systems. We expect our simpler approach to not affect gross qualitative features associated with the influence of inter-pulse separation time Δt on the evolution of geometrical phase. This critical aspect remains the focus of our study of dynamic decoupling pulses on geometrical phases in this section.

Lastly we note that the choice of a measurable quantity as a substitute for geometrical phase η is a difficult one to make as generally it is not easy to detect geometric phases using experimental techniques. This is mainly due to limitations associated with adiabatic conditions as well as the geometric nature of the evolution of the quantum system. However, in the case of solid state excitations like excitons formed in quantum dots, multi-wave mixing techniques [35] can provide a possible route to observing geometric phases despite weak photon-echo signals which are obtained under current experimental arrangements [35].

6. Conclusions

We have studied the effect of phonon mediated interactions on the non-unitary evolution of the geometrical phase in excitonic qubits systems. We have examined the response of the geometric phase to changes in temperature, external electric field E and quantum dot parameters for two mechanisms of exciton–phonon interaction which involve deformation potential and piezoelectric coupling. We have also investigated the effect of dynamic decoupling in the form of equidistant ideal π-pulses on the evolution of geometrical phase in the presence of decoherence effects.

Our results show significant differences in the response of geometric phases to changes in temperature, for the two mechanisms of exciton–phonon interaction involving deformation potential and piezoelectric coupling. Thermal effects appear to play a relatively minor role in the case of phonon coupling via the piezoelectric mechanism. However due to the presence of both coupling mechanisms in solid state systems, one can conclude that bath temperatures play a critical role in increasing decoherence effects depending on the bias, external electric field, quantum dot size and interdot distances in excitonic quantum dots that are entangled by Förster coupling. On the other hand, zero point fluctuations become increasingly important for small quantum dot sizes at very low temperatures. We also expect spontaneous emission processes to provide an important alternative route to decoherence in quantum dot systems coupled to photon modes. While we have not fully incorporated this mechanism of decoherence in our calculations of the geometric phase, we expect exciton decay processes to be just as important as phonon mediated interactions, especially at low temperatures.

In the presence of time-reversal operations involving π-pulses, our results are consistent with those of earlier works showing the reduction of undesirable thermal effects even at relatively high temperatures $\approx$100 K. Our results show that dynamic decoupling via π-pulses becomes most effective in reducing decoherence including zero point fluctuations at pulse interval $\Delta t \approx 0.1$–0.5 ps. This timescale is consistent with the phonon reservoir correlation time for the GaAs/AlGaAs material system.

Finally, our results indicate that thermal effects associated with phonon mediated interactions exert a measurable influence on the non-unitary evolution of the geometrical phase in quantum dot systems for a selected range of external parameters. Dynamic decoupling via π-pulses appears to reduce the undesirable effects of an increasing bath temperature and possibly provide a viable solution to the physical realization of logic systems based on geometric phase gates.

References

[1] Loss D and DiVincenzo D P 1998 *Phys. Rev.* A **57** 120
[2] Biolatti E, Iotti R C, Zanardi P and Rossi F 2000 *Phys. Rev. Lett.* **85** 5647
[3] Li X, Wu Y, Steel D, Gammon D, Stievater T H, Katzer D S, Park D, Piermarocchi C and Sham L J 2003 *Science* **301** 809
[4] Krenner H J, Stufler S, Sabathil M, Clark E C, Ester P, Bichler M, Abstreiter G, Finley J J and Zrenner A 2005 *New J. Phys.* **7** 184
[5] Bayer M, Hawrylak P, Hinzer K, Fafard S, Korkvsinki M, Wasilewski Z R, Stern O and Forchel A 2001 *Science* **291** 451
[6] Muller A, Wang Q Q, Bianucci P, Shih C K and Xue Q K 2004 *Appl. Phys. Lett.* **84** 981
[7] Zrenner A, Beham E, Stufler S, Findeis F, Bichler M and Abstreiter G 2002 *Nature* **418** 612
[8] Stievater T H, Xiaoqin Li, Steel D G, Gammon D, Katzer D S, Park D, Piermarocchi C and Sham L J 2001 *Phys. Rev. Lett.* **87** 133603
[9] Lidar D A, Chuang I L and Whaley K B 1998 *Phys. Rev. Lett.* **81** 2594
[10] Zanardi P and Rasetti M 1997 *Phys. Rev. Lett.* **79** 3306
[11] Hohenester U 2006 *Phys. Rev.* B **74** 161307(R)
[12] Xue P and Xiao Y F 2006 *Phys. Rev. Lett.* **97** 140501
[13] Zanardi P 1999 *Phys. Lett.* A **258** 77
[14] Falci G, Fazio R, Palma G M, Siewet J and Vedral V 2000 *Nature* **407** 355
[15] Solinas P, Zanardi P, Zanghi N and Rossi F 2003 *Phys. Rev.* B **67** 121307(R)
[16] Berry M V 1984 *Proc. R. Soc.* A **392** 45
[17] Zhu S L and Zanardi P 2005 *Phys. Rev.* A **72** 020301(R)
[18] Tong D M, Sjöqvist E, Kwek L C and Oh C H 2004 *Phys. Rev. Lett.* **93** 080405
[19] Yi X X, Tong D M, Wang L C, Kwek L C and Oh C H 2006 *Phys. Rev.* A **73** 052103
[20] Lombardo F C and Villar P I 2006 *Phys. Rev.* A **74** 042311
[21] Yi X X, Wang L C and Zheng T Y 2004 *Phys. Rev. Lett.* **92** 150406
[22] Yuan X Z and Zhu K D 2006 *Phys. Rev.* B **74** 073309
[23] Tian M, Barber Z W, Fisher J A and Babbit Wm R 2004 *Phys. Rev.* A **69** 050301
[24] Leek P J *et al* 2007 *Science* **318** 1889
[25] Möttönen M, Vartiainen J J and Pekola J P 2008 *Phys. Rev. Lett.* **100** 177201
[26] Whitney R S, Makhlin Y, Shnirman A and Gefen Y 2005 *Phys. Rev. Lett.* **94** 070407
[27] Chiara G and Palma M G 2008 *Int. J. Theor. Phys.* **47** 2165
[28] Nazir A, Spiller T P and Munro W J 2002 *Phys. Rev.* A **65** 042303
[29] Rezakhani A T and Zanardi P 2006 *Phys. Rev.* A **73** 052117
[30] Nazir A, Lovett B W and Briggs G A D 2004 *Phys. Rev.* A **70** 052301
[31] Viola L and Lloyd S 1998 *Phys. Rev.* A **58** 2733
[32] Ban M 1998 *J. Mod. Opt.* **45** 2315
[33] Akira M 1980 *Phys. Rev.* B **21** 2051
[34] Bolton S R, Neukirch U, Sham L J, Chemla D S and Axt V M 2002 *Phys. Rev. Lett.* **85** 2002
[35] Kishimoto T, Takahashi H, Hasegawa A, Sasaki M and Minami F 2008 *J. Lumin.* **128** 1075
[36] Uhrig G S 2007 *Phys. Rev. Lett.* **98** 100504
[37] Franceschetti A and Zunger A 1997 *Phys. Rev. Lett.* **78** 915
[38] Silverman K L, Mirin R P, Cundiff S T and Norman A G 2003 *Appl. Phys. Lett.* **82** 4552
[39] Nazir A, Lovett B W, Barrett S D, Reina J H and Briggs G A D 2005 *Phys. Rev.* B **71** 045334
[40] Thilagam A and Lohe M A 2008 *J. Phys.: Condens. Matter* **20** 315205
[41] Thilagam A and Lohe M A 2006 *J. Phys.: Condens. Matter* **18** 3157
[42] Takagahara T 1985 *Phys. Rev.* B **31** 6552
[43] Leggett A J, Chakravarty S, Dorsey A T, Fisher M P A, Garg A and Zwerger W 1987 *Rev. Mod. Phys.* **59** 1
[44] Shiokawa K and Lidar D A 2004 *Phys. Rev.* A **69** 030302
[45] Haug H and Jauho A P 1996 *Quantum Kinetics in Transport and Optics of Semiconductors* (Heidelberg: Springer)